

Metabolomics Study on the Therapeutic Mechanism of *Schisandra chinensis* Polysaccharides on Concanavalin A-Induced Immunological Liver Injury in Mice

Lihua Chen, Yingying Shan¹, Chunmei Wang¹, He Li¹, Jianguang Chen¹, Jinghui Sun¹

Editorial Board of Journal of Beihua University, Beihua University, ¹College of Pharmacy, Beihua University, Jilin, China

Submitted: 13-Jun-2020

Revised: 30-Jul-2020

Accepted: 24-Feb-2021

Published: 12-Jul-2021

ABSTRACT

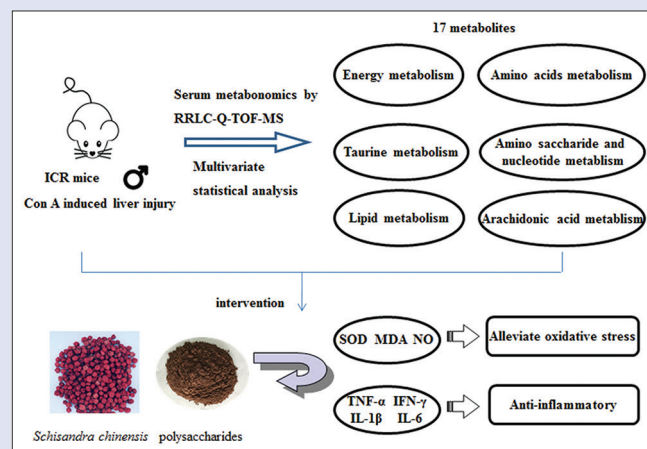
Background: *Schisandra chinensis* is a traditional Chinese herbal medicine which protects hepatic function. Its primary component is polysaccharides which is used in the treatment of hepatic injury, but the mechanism of action of *S. chinensis* polysaccharides (SCP) in immunological liver injury induced by concanavalin A (Con A) is still not clear. **Aim:** In this study, we aimed to evaluate the hepatoprotective mechanism of SCP in immunological liver injury. **Subjects and Methods:** In this study, we performed rapid-resolution liquid chromatography coupled with quadruple-time-of-flight mass spectrometry-based serum metabolomics approach to investigate the hepatoprotective effects of SCP against Con A-induced immunological liver injury in mice. **Results:** According to our results, SCP significantly increased the activity of superoxide dismutase in the liver; decreased the level of serum aspartate aminotransferase (AST), serum alanine aminotransferase (ALT), tumor necrosis factor- α , interferon- γ , interleukin (IL)-1 β , and IL-6 in the serum, and decreased the level of malondialdehyde and nitric oxide in the liver of mice with immunological liver injury induced by Con A. In this study, we identified 17 biomarkers through metabolomic analysis, and after the administration of SCP, 16 of them were found to return to the normal levels. Our analysis suggested that some metabolic pathways are involved in the mechanisms of action of SCP for the treatment of the immunological liver injury, including energy metabolism, amino acid metabolism, taurine metabolism, amino saccharide and nucleotide metabolism, arachidonic acid metabolism, and lipid metabolism. **Conclusion:** SCP could alleviate the oxidative stress and inflammatory reaction in the immunological liver injury and recover the metabolic dysfunction caused by Con A.

Key words: Immunological liver injury, metabolomics, polysaccharides, rapid resolution liquid chromatography coupled with quadruple-time-of-flight mass spectrometry, *Schisandra chinensis*

SUMMARY

- *Schisandra chinensis* (Turcz.) Baill is a traditional Chinese medicine and is widely used for the treatment of liver injury in East Asian regions. Polysaccharides are the primary components of *Schisandra chinensis*.
- An LC/MS-based metabolomics method was used to identify the metabolic regulation of SCP on the immunological liver injury induced by Con A in mice.
- After metabolomic analysis, 17 biomarkers were identified and 16 of them were found to return to normal levels after the administration of SCP.

- *Schisandra chinensis* polysaccharides could alleviate the oxidative stress and inflammatory reaction in the immunological liver injury and recover the metabolic dysfunction caused by Con A.



Abbreviations used: SCP: *Schisandra chinensis* polysaccharides; Con A: Concanavalin A; RRLC-Q-TOF-MS: Rapid-resolution liquid chromatography coupled with quadruple-time-of-flight mass spectrometry; ALT: Alanine aminotransferase; AST: Aspartate aminotransferase; TNF- α : Tumor necrosis factor- α ; IFN- γ : Interferon- γ ; IL-1 β : Interleukin 1 β ; IL-6: Interleukin 6; MDA: Malondialdehyde; NO: Nitric oxide; SOD: Superoxide dismutase; PCA: Principal component analysis; OPLS-DA: Orthogonal partial least squares discrimination analysis.

Correspondence:

Dr. Jinghui Sun,
College of Pharmacy, Beihua University, 3999
Binjiang East Road, Jilin 132013, China.
E-mail: sunjinghui2008@126.com
DOI: 10.4103/pm.pm_255_20

Access this article online

Website: www.phcog.com

Quick Response Code:



INTRODUCTION

Immunological liver injury is an important factor that can cause acute liver failure, which is characterized by many inflammatory cells infiltrating in the liver tissue and the occurrence of immune inflammatory response.^[1] Inflammatory response is the primary cause of many liver diseases, even liver parenchyma. Immunological liver injury is an event leading to liver fibrosis, cirrhosis, and even liver tumors, which may determine the development of liver diseases.^[2]

Schisandra chinensis (Turcz.) Baill is a traditional Chinese medicine and is widely used in the East Asian regions. It shows multiple

This is an open access journal, and articles are distributed under the terms of the Creative Commons Attribution-NonCommercial-ShareAlike 4.0 License, which allows others to remix, tweak, and build upon the work non-commercially, as long as appropriate credit is given and the new creations are licensed under the identical terms.

For reprints contact: WKHLRPMedknow_reprints@wolterskluwer.com

Cite this article as: Chen L, Shan Y, Wang C, Li H, Chen J, Sun J. Metabolomics study on the therapeutic mechanism of *Schisandra chinensis* polysaccharides on concanavalin A-induced immunological liver injury in mice. Phcog Mag 2021;17:293-301.

pharmacological effects, especially in the liver. Our previous work has shown that polysaccharides are the primary components of *S. chinensis* which are responsible for the recovery of the liver from any metabolic injury such as chemical, alcoholic, and fatty liver conditions.^[3,4] However, the hepatoprotective action of *S. chinensis* polysaccharides (SCP) in immunological liver injury has not been fully clarified. Therefore, in this study, we aimed at investigate the hepatoprotective effect of SCP against the Concanavalin A (Con A)-induced immunological liver injury in mice by using a serum metabolomics approach based on the rapid resolution liquid chromatography coupled with quadruple-time-of-flight mass spectrometry (RRLC-Q-TOF-MS).

SUBJECTS AND METHODS

Chemicals and reagents

The following chemicals were obtained: Con A for injection (IV grade, Sigma, Louis, USA); kits for the detection of serum alanine aminotransferase (ALT), serum aspartate aminotransferase (AST), superoxide dismutase (SOD), malondialdehyde (MDA), and nitric oxide (NO) (Nanjing Jiancheng Bioengineering Institute, Nanjing, China); interleukin (IL)-1 β , IL-6, tumor necrosis factor (TNF)- α , and interferon (IFN)- γ enzyme-linked immunosorbent assay (ELISA) kits (Shanghai Lengton Bioscience Co, Ltd., Shanghai, China); acetonitrile and methanol (high-performance liquid chromatography (HPLC)-grade, TEDIA, Cincinnati, USA). Ultrapure water used in the HPLC experiments was purified using a Milli-Q Ultra-pure water system (Millipore, Billerica, USA).

Preparation of *Schisandra chinensis* polysaccharides

S. chinensis was identified by Professor Wei Wang (College of Pharmacy, Beihua University) and was provided by Jian Schisandra Seedlings Base of Jilin Province. SCP was prepared by the Pharmaceutical Experimental Center of Beihua University, and the method of preparation has been reported in our previous publication.^[4] Water-soluble crude SCP was extracted through water extraction and alcohol precipitation method, with a yield of 8.55%. The total carbohydrate content of SCP was measured by phenol-sulfuric acid method, in which glucose was taken as the standard.^[5] Uronic acid was measured by M-hydroxydiphenyl method and D-galactose was used as the standard.^[6] Protein was measured by Bradford method,^[7] and the composition of monosaccharides was measured by HPLC.^[8] According to our results, the contents of the total sugar, uronic acid, and protein in SCP were 40.60%, 24.70%, and 1.51%, respectively. The content of monosaccharides was 38.00% (glucose), 36.70% (galactose), 12.00% (galacturonic acid), 7.30% (arabinose), 4.00% (rhamnose), 1.20% (mannose), and 0.60% (glucuronic acid).

Animal handling

Male imprinting control region mice, 6 weeks old, were purchased from Changchun Yisi Experimental Animal Technology Co., Ltd. (Changchun, China, No. SCXX [ji] 2018-0007). The mice were raised in a clean laboratory room with good ventilation and were not restricted to eat and drink. The temperature of the laboratory room maintained from

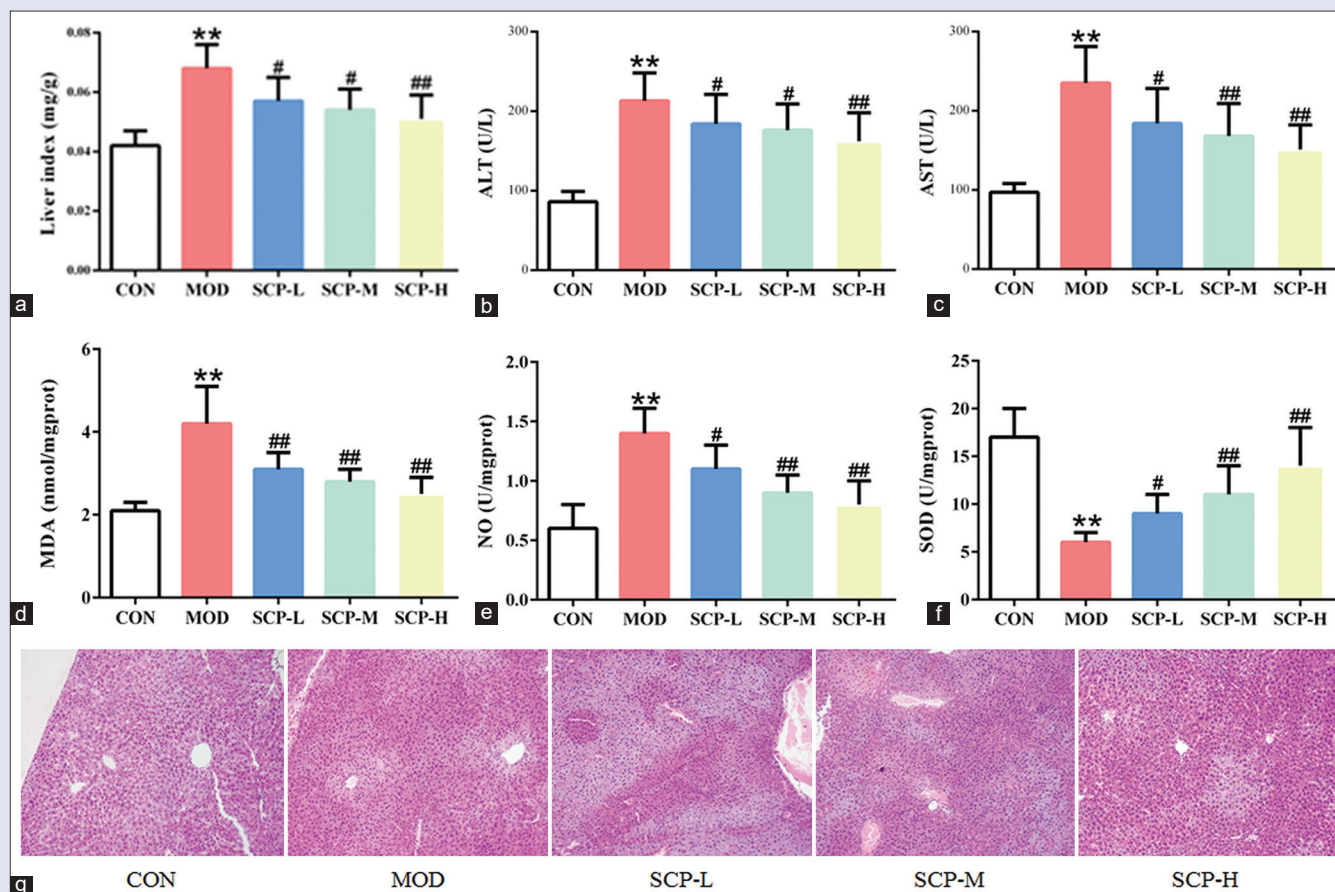


Figure 1: Effects of *Schisandra chinensis* polysaccharides on liver indexes (a), AST (b), ALT (c), Malondialdehyde (d), NO (e), Superoxide dismutase (f) levels and histomorphological changes of the liver (g)

18°C to 22°C, and the relative humidity was maintained at 45%–55%, and the mice were fed on a normal diet. The experimental procedures were approved by Beihua University Laboratory Animal Ethics Committee (No. 20190013).

A total of 75 mice were divided into five groups: control group (CON), model group (MOD), 20 mg/kg SCP group (SCP low dose, SCP-L), 40 mg/kg SCP group (SCP medium-dose, SCP-M), and 80 mg/kg SCP group (SCP high dose, SCP-H), with 15 mice in each group. The corresponding doses of SCP aqueous solution were intragastrically administered to mice in SCP-L, SCP-M, and SCP-H groups, respectively. CON and MOD groups were administered with an equal volume of distilled water. The administration was continued for duration of 21 days. Con A (40 mg/kg) was administered to the mice in MOD and SCP-treated groups on the 20th day, and an equal volume of normal saline was administered to those in CON group through tail intravenous injection. Eight hours after the injection of Con A, ether was used to anesthetize the mice. Blood sample was collected by eye extraction and centrifuged at 3000 rpm for 10 min for collecting

the serum. Then, the mice were sacrificed through CO₂ inhalation, and their organs (liver, spleen, and thymus) were harvested, and the liver, spleen, and thymus and serum samples were stored at –80°C.

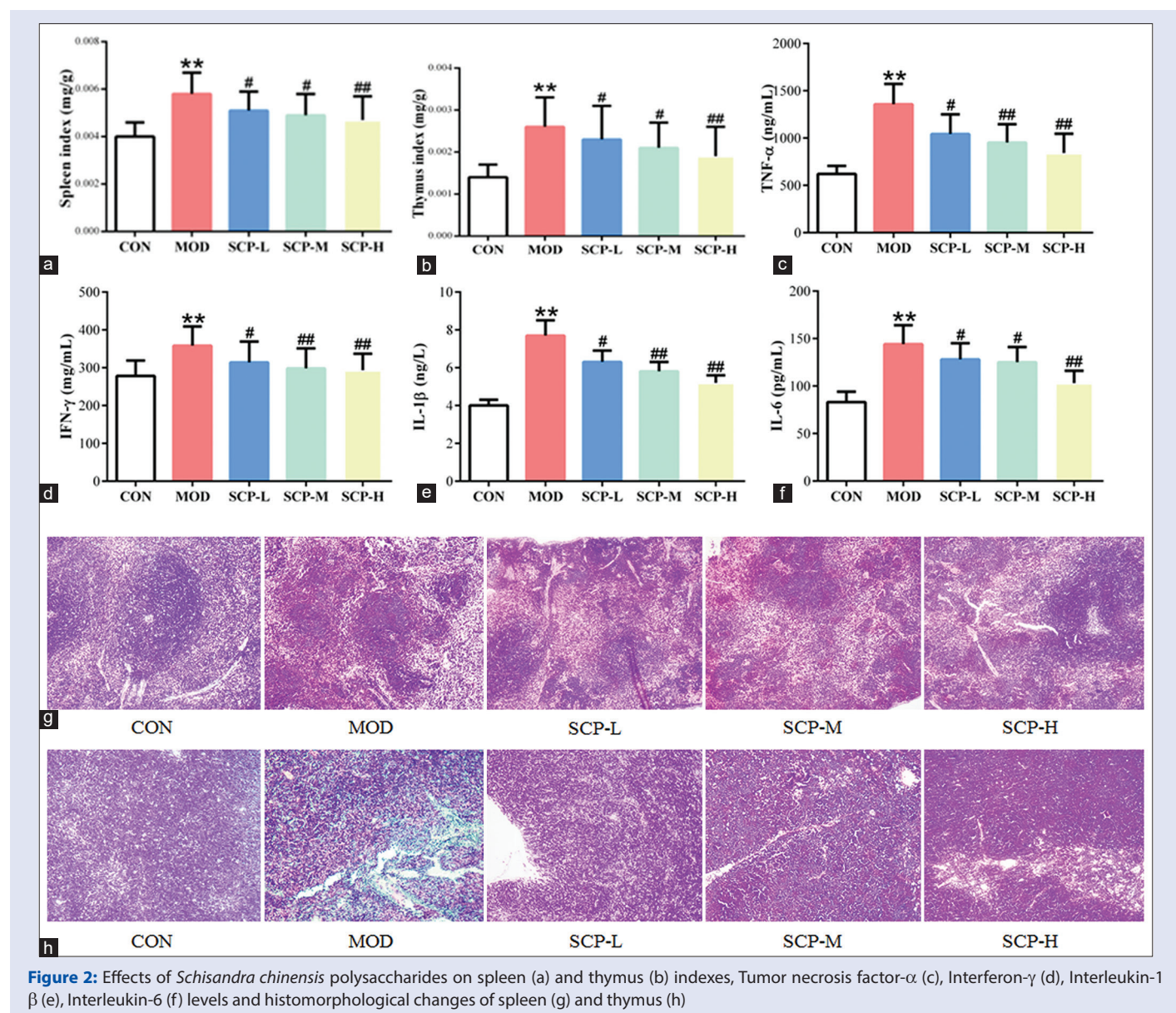
Determination of organ indexes and histomorphology

The organ indexes of the thymus, liver, and spleen of mice were calculated as follows:

$$OI = OW/BW$$

Where OI represents organ index, OW represents organ weight, and BW represents body weight.

The samples of liver, spleen, and thymus were fixed in 10% formaldehyde for 24 h. From these samples, 5 μm thin slices were cut using a microtome for the histopathological analysis. H and E staining (H and E) method was used to stain the slices for 10 min, and stained slices were sectioned routinely. The liver, spleen, and thymus sections were examined under an optical microscope (magnification, ×100).



Determination of serum ALT, aspartate aminotransaminase, interferon- γ , tumor necrosis factor- α , interleukin-6, and interleukin-1 β

The activities of serum AST and ALT were analyzed following the instructions of the commercial kits. The levels of IFN- γ , TNF- α , IL-1 β , and IL-6 were detected in the serum with the ELISA method.

Determination of nitric oxide, malondialdehyde, and superoxide dismutase

Briefly, 0.2 g of the left lobe of the liver was added to nine times the volume of saline in an ice water bath for the preparation of a 10% liver tissue homogenate, and the homogenate was centrifuged to obtain the supernatant. NO and MDA levels and SOD activity in the supernatant were measured by following the instructions provided in the kit.

Resolution liquid chromatography coupled/mass spectrometry analysis

For RRLC/MS, 1 mL methanol was added to 100 μ L of serum sample and vortexed for 30 s. The samples were centrifuged (12,000 rpm, 4°C and 5 min) and the supernatant was obtained. After filtering through a 0.45 μ m filter, the filtrate was transferred to a clear Eppendorf tube and stored at 4°C for further use.

A 1200 rapid resolution liquid chromatographic system (Agilent, USA) was used for the RRLC analysis. A 5 μ L aliquot of the sample solution was injected into the Agilent SB-C₁₈ column (100 mm \times 3.0 mm, 1.8 μ m) for elution, in which the temperature was maintained at 25°C, the mobile phase was 0.1% formic acid (A) and acetonitrile (B). The elution

conditions were as follows: 0–10 min, 5%–50% B and 10–20 min, 50%–95% B, and the flow rate was 300 μ L/min.

For the MS analysis, we used 6520 Q-TOF MS (Agilent, USA) in both positive and negative modes, in which the scan range was maintained at 50–1000 m/z , the drying gas (N_2) temperature was maintained at 350°C, the capillary voltage was set to 3.5 kV, the flow rate was maintained at 8.0 L/min, the nebulizer was set at 207 kPa, and the fragmentor and skimmer were set at 175 V and 65 V, respectively.

Analysis and identification of metabolites

We analyzed the raw data using Mass Hunter software (version B.03.01, Agilent, USA) to obtain a list of retention time, mass, and absorption peak area. Mass Profiler Professional (version B.02.02, Agilent, Santa Clara, CA, USA) software was used for filtration and normalization. The resultant data were introduced to Simca-P software (version B.14.1, Umetrics, Sweden) for the multivariate analysis. The general separation of all samples was observed by the principal component analysis (PCA) at first. Orthogonal partial least squares discrimination analysis (OPLS-DA) was used to build and utilize a model to identify the differential metabolites among groups. The identification and elucidation of structure of differential metabolites were performed by the MS/MS analysis by comparing the molecular weight, retention time, and molecular characterization of fragmented ions. Available biochemical databases were also interpreted for the identification, such as Human Metabolome Database (HMDB)(<http://www.hmdb.ca>), LIPID MAPS (<http://www.lipidmaps.org>), and Kyoto Encyclopedia of Genes and Genomes (<http://www.genome.jp/kegg>).

Statistical analysis

The data were calculated as mean \pm standard deviation, and “n” denotes the number of samples in each group. The data were analyzed by the

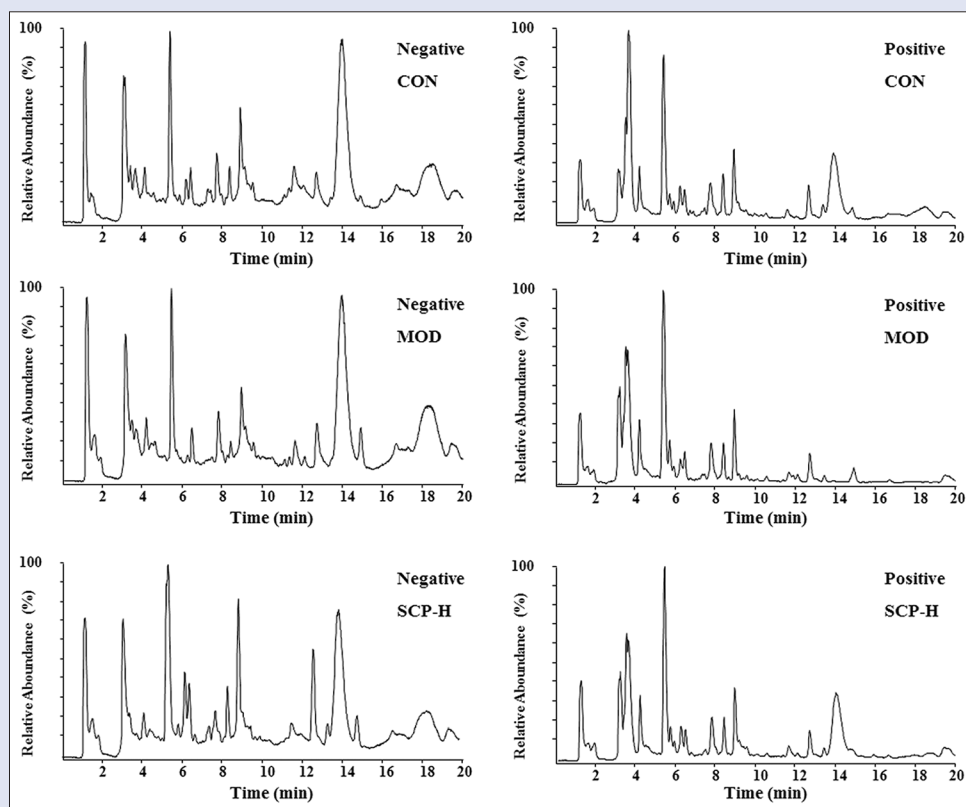


Figure 3: Base peak intensity chromatograms obtained from negative and positive ion Rapid resolution liquid chromatography coupled with quadruple-time-of-flight mass spectrometry analyses of CON, MOD and *Schisandra chinensis* polysaccharides-H mice

one-way analysis of variance (SPSS 20.0 (IBM SPSS Inc., Chicago, IL, USA)), and a $P < 0.05$ was considered statistically significant in statistics.

RESULTS

Effects of *Schisandra chinensis* polysaccharides on immunological liver injury in mice

The liver index and the activity of ALT and AST and levels of MDA and NO in the liver tissue of mice in MOD group were significantly higher than those in the CON group ($P < 0.01$), and the activity of SOD in the liver tissue of mice in MOD group was significantly lower than that in the CON group ($P < 0.01$). The pathological results showed that the edema and local necrosis of hepatocytes, and the dilatation and hyperemia of central vein could be seen, which were mainly located around the central vein in MOD group, indicating that the mouse immunological liver injury model induced by Con A was successfully built. The liver index and activity of ALT and AST and levels of MDA and NO levels in the liver tissue of mice in SCP-treated groups were significantly lower than those in MOD group ($P < 0.05$ and $P < 0.01$), and the SOD activities in SCP-treated groups were significantly higher than those in the MOD group ($P < 0.05$ and

$P < 0.01$), and the structure of hepatic lobules was almost normal and the hepatic sinusoidal congestion was significantly alleviated in SCP-treated groups [Figure 1].

Effects of *Schisandra chinensis* polysaccharides on interleukin-1 β , interleukin-6, interferon- γ , and tumor necrosis factor- α levels and immune organs

The spleen and thymus indexes and the serum IL-1 β , IL-6, TNF- α , and IFN- γ contents in the MOD group were significantly higher than those in CON group ($P < 0.01$). The spleen and thymus indexes and the serum IL-1 β , IL-6, TNF- α , and IFN- γ contents in SCP-treated groups were significantly lower than those in the MOD group ($P < 0.05$ and $P < 0.01$) [Figure 2]. According to our results, in contrast to those in the CON group, the number and the volume of splenic corpuscles and the number of lymphocytes in the thymus were decreased. Furthermore, the boundaries between the medulla and cortex were unclear, and the volumes of medulla were decreased in MOD group. In the SCP-treated groups, the number of splenic corpuscles in the membranous area decreased slightly, and the medullary and cortical structures were clear. In addition, the boundaries between the medulla

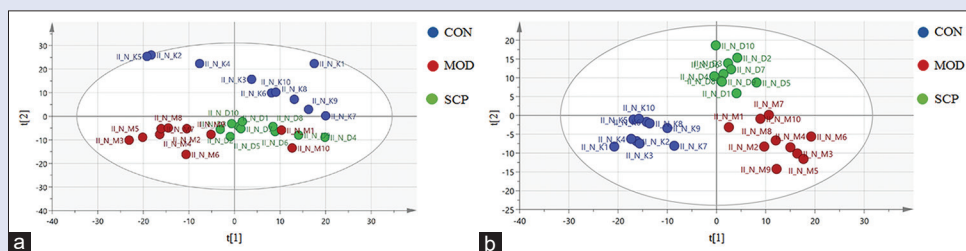


Figure 4: Principal component analysis score plots from serum sample of CON, MOD and *Schisandra chinensis* polysaccharides-H mice in positive (a) and negative (b) ion mode

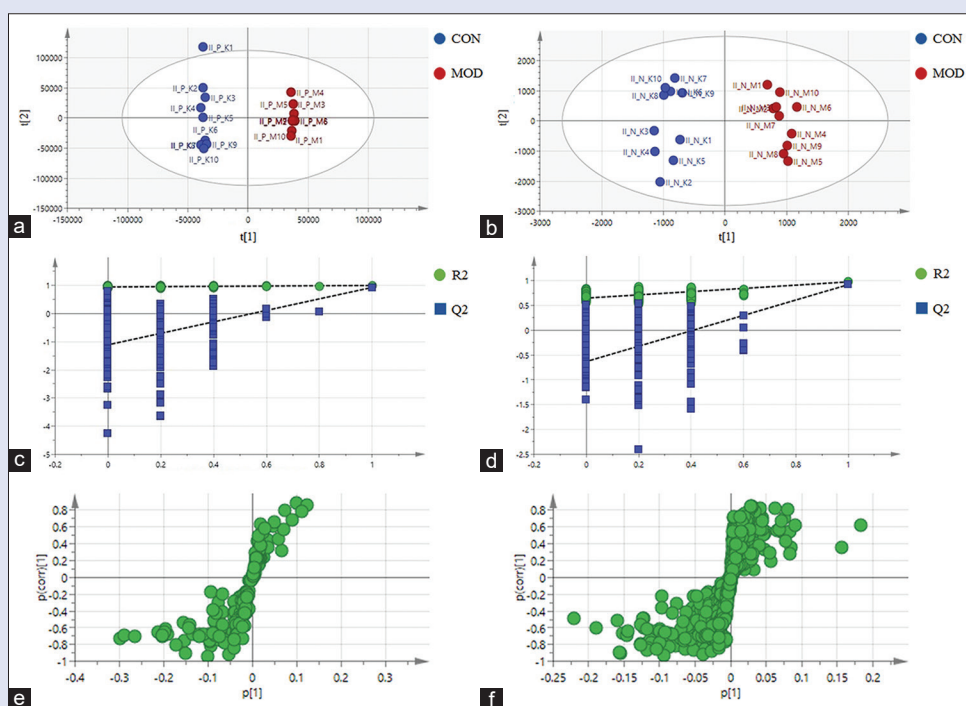


Figure 5: Orthogonal partial least squares discrimination analysis from the serum sample of CON and MOD mice. Score plot in positive (a) and negative (b) ion mode. Permutation test for the validity of model in positive (c) and negative (d) ion mode. Loading plot in positive (e) and negative (f) ion mode

and cortex were distinct and the number of lymphocytes was normal in contrast to those in the MOD group [Figure 2].

Con A induces excessive proliferation of lymphocytes which leads to a massive production of pro-inflammatory factors, including IL-1 β , IL-6, and TNF- α , which further promote the release of the downstream inflammatory factor such as TNF- α . The activated immune cells can increase the immune response and the enlargement of spleen and thymus, and subsequently many activated immune cells accumulate in the liver, resulting in the enlargement and injury of the liver. This may

increase the permeability of the cell membrane, thereby releasing ALT and AST in the blood stream.^[9,10]

Serum metabolomics analysis

Figure 3 shows the base peak intensity chromatograms of serum samples of mice in CON, MOD, and SCP-H groups, and the potential metabolites of the serum samples were identified through PCA according to the RRLC-Q-TOF-MS data. PCA is a common unsupervised method used in the analysis of multivariate data, and it is often used to reduce

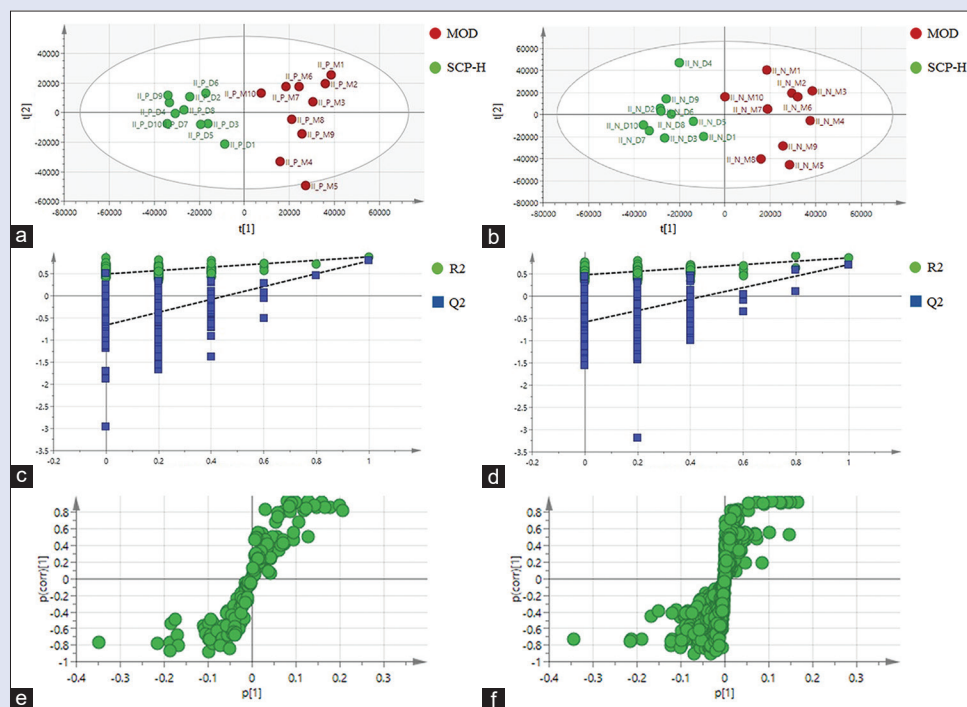


Figure 6: Orthogonal partial least squares discrimination analysis from serum sample of MOD and *Schisandra chinensis* polysaccharides-H mice. Score plot in positive (a) and negative (b) ion mode. Permutation test for the validity of model in positive (c) and negative (d) ion mode. Loading plot in positive (e) and negative (f) ion mode

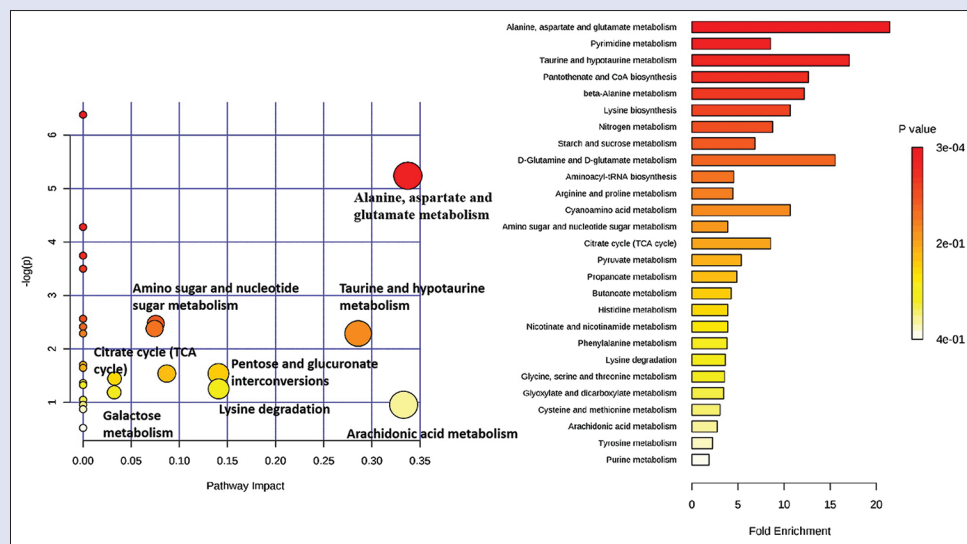


Figure 7: The metabolic pathway analysis based on Rapid resolution liquid chromatography coupled with quadruple-time-of-flight mass spectrometry analysis of biomarkers in serum of mice treated with *Schisandra chinensis* polysaccharides

the dimensionality with a minimal information loss but retaining the characteristics which can contribute most to the variance. It was found that the scattered points of CON, MOD, and SCP-H samples showed a significant separation in both negative and positive ion mode [Figure 4, PCA score plots].

As a supervised method, OPLS-DA was used to analyze the data from two groups to obtain the score charts, and the results suggested that there was a significant difference between CON and MOD groups, as well as between MOD and SCP-H groups, and the validity of the model was

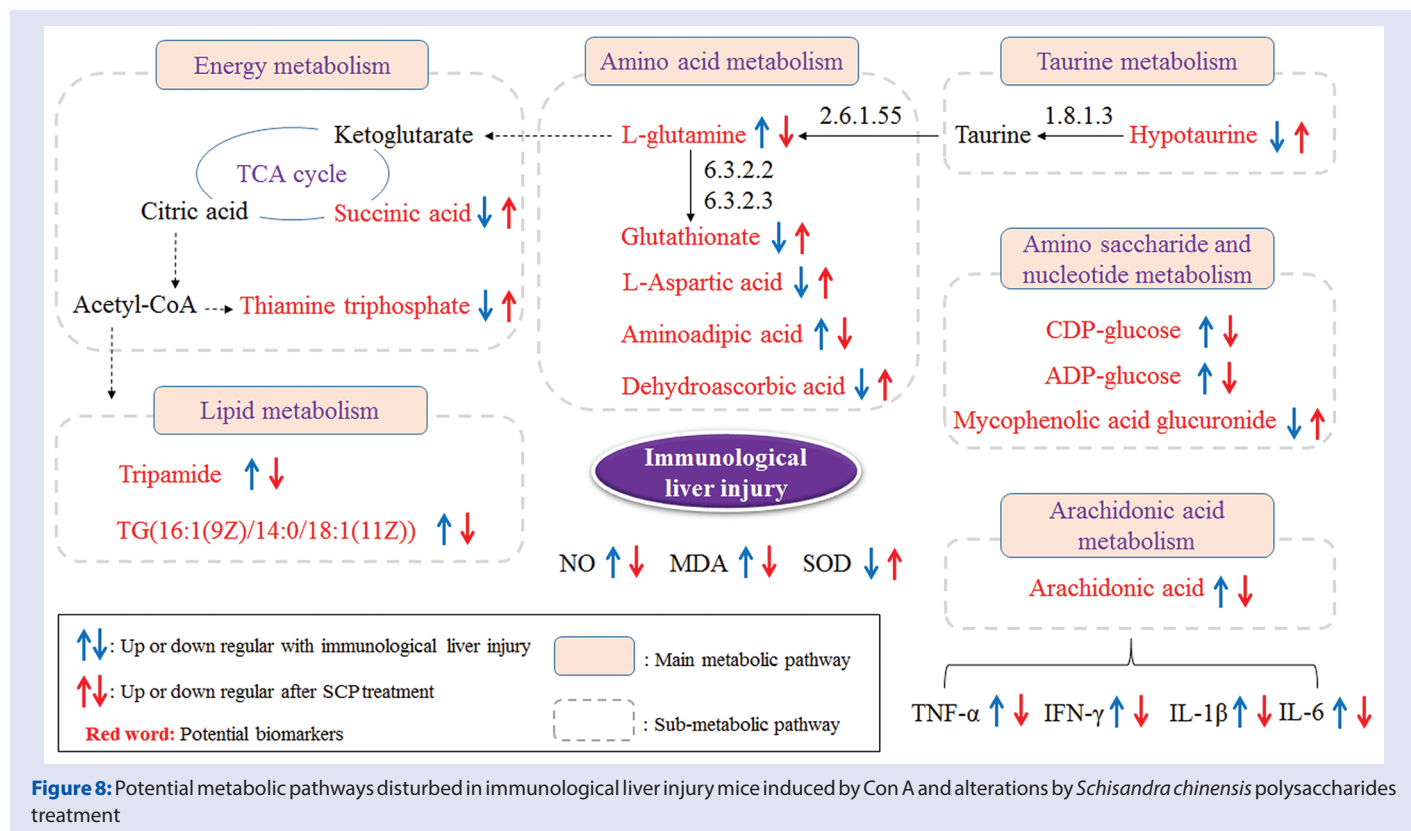
evaluated by permutation test ($n = 200$). The results showed that the R^2Y and Q^2 both were larger than 0.5 and close to 1, indicating that model had a good fit [Figures 5 and 6].

OPLS-DA was used to analyze the data for screening potential biomarkers to confirm the differences of endogenous metabolites in the serum of mice. The results have been shown as OPLS-DA loading plots. The potential biomarkers were chosen according to the VIP values obtained by OPLS-DA, in which the variables with $VIP > 1$ and $P < 0.05$ by Student's t -test were regarded as the potential biomarkers. Accordingly,

Table 1: Data of identified metabolites detected by rapid resolution liquid chromatography coupled with quadruple-time-of-flight mass spectrometry

Ion mode	Metabolite	Mass	Molecular formula	Related pathway	Changes (C/M)	Changes (M/S)	
Positive	L-Aspartic acid	133.10	$C_4H_7NO_4$	Aspartic acid metabolism	↓	↑	
	Acetylphosphate	140.03	$C_2H_5O_5P$	Pyruvate metabolism	↓	-	
	Uracil	112.09	$C_4H_4N_2O_2$	Pyrimidine metabolism	↓	↑	
	Cytosine	111.10	$C_4H_5N_3O$	Pyrimidine metabolism	↓	↑	
	Hypotaurine	109.15	$C_2H_7NO_2S$	Taurine metabolism	↓	↑	
	Mycophenolic acid glucuronide	496.46	$C_{23}H_{28}O_{12}$	Carbohydrate metabolism	↓	↑	
	Dehydroascorbic acid	174.11	$C_6H_6O_6$	Amino acid metabolism	↓	↑	
	Amino adipic acid	161.16	$C_6H_{11}NO_4$	Amino acid metabolism	↑	↓	
	L-Glutamine	146.14	$C_5H_{11}N_2O_3$	Amino acid metabolism	↑	↓	
	Arachidonic acid	304.47	$C_{20}H_{32}O_2$	Arachidonic acid metabolism	↑	↓	
	Succinic acid	118.09	$C_4H_6O_4$	Tricarboxylic acid cycle	↓	↑	
	Negative	CDP-glucose	565.32	$C_{15}H_{25}N_3O_{16}P_2$	Amino saccharide and nucleotide metabolism	↑	↓
		ADP-glucose	589.34	$C_{16}H_{25}N_5O_{15}P_2$	Amino saccharide and nucleotide metabolism	↑	↓
		Tripamide	369.87	$C_{16}H_{20}N_3O_3S$	Lipid metabolism	↑	↓
TG (16:1 (9Z)/14:0/18:1 (11Z))		803.31	$C_{51}H_{94}O_6$	Lipid metabolism	↑	↓	
Thiamine triphosphate		505.29	$C_{12}H_{20}N_4O_{10}P_3S$	Tricarboxylic acid cycle	↓	↑	
Glutathionate		307.32	$C_{10}H_{17}N_3O_6S$	Tricarboxylic acid cycle	↓	↑	

M-C represented MOD group versus CON group; S-M represented SCP-H group versus MOD model group. "↑" and "↓" indicated that the metabolite was up- and down-regulated; "-" indicated that the metabolite did not significantly change. CON: Control group; MOD: Model group; SCP: *Schisandra chinensis* polysaccharides; CDP: Cytidine diphosphate; ADP: Adenosine diphosphate; TG: Triglyceride



there were a total of 17 potential biomarkers with significant differences between CON and MOD groups, of which 16 were significantly different between MOD and SCP-H groups [Table 1].

The HMDB ID of metabolites was input into Metabo Analyst software (<http://www.metaboanalyst.ca/MetaboAnalyst>) for the enrichment analysis. Based on the *P* value of the relevant pathway (*Y* axis) and impact value of topological analysis (*X* axis), there were five pathways (amino acid metabolism, taurine metabolism, tricarboxylic acid (TCA) cycle, arachidonic acid metabolism, and amino saccharide and nucleotide metabolism) were selected as the primary pathways through which SCP was considered to alleviate Con A-induced immunological liver injury in mice [Figure 7].

DISCUSSION

It is believed that oxidative stress may play an important role in immunological liver injury, in which NO is a typical free radical under *in vivo* conditions and acts as a neurotransmitter to mediate the immune response.^[11] SOD with a significant antioxidative property can eliminate the excessive free radicals in the body to alleviate the liver injury in mice.^[12] MDA can destroy the structure of the cell membrane, thereby causing the cells to swell and necrotize; therefore, it can reflect the degree of cell injury induced by peroxidation.^[13] In this study, the results showed that SCP markedly inhibited the Con A-induced elevation of the serum IL-1 β , IL-6, TNF- α , and IFN- γ levels, confirming the anti-inflammatory activity of SCP in immunological liver injury mice. However, the protection of SCP against the immunological liver injury may be related to its antioxidative effect. Based on the most significant therapeutic effect shown in SCP-H group, the serum samples of mice in SCP-H group were selected for the metabolomics study.

TCA cycle is a common metabolic pathway in aerobic organisms which provides energy to the organism based on the final metabolic pathway of carbohydrates, lipids, and amino acids – the three major nutrients in the body. In the process of immunological liver injury, due to the damage of mitochondrial function, excessive free radicals of oxygen are produced, which reduces the production of ATP.^[14] Succinic acid, glutathione, and thiamine triphosphate are the intermediates in the TCA cycle, whose levels were significantly reduced in the MOD group. However, in the SCP group, there was a significant increase in the levels of the aforementioned metabolites, indicating that SCP alleviates the energy metabolism disorders. The conjugation of glucuronic acid, synthesized by a series of catalytic reactions of uridine diphosphate glucose, is a major pathway of phase II metabolism in liver, and it can also enter pentose phosphate pathway to provide energy for the body. In this study, the abnormal increasing levels of CDP-and ADP-glucose and decreasing levels of mycophenolic acid glucuronide in the MOD group were alleviated by SCP. These results indicate that SCP improves the liver injury and the disorder of glucose utilization in the immunological liver injury.

Taurine is an essential amino acid mainly synthesized by the liver, with the protective effect of reducing liver steatosis and lipid peroxidation.^[15] When an inflammatory reaction occurs in the liver, the synthesis of taurine is reduced and its antioxidant effect is correspondingly weakened.^[16] The level of hypotaurine (the precursor of taurine) in MOD group was significantly lower than that in the CON group, which was significantly alleviated by SCP.

Liver is the primary organ for the amino acid metabolism, which gets hampered when there is injury to the liver.^[17] Amino adipic acid is the intermediate compound of lysine and glycopurine metabolism. Glutamine (Gln), the most abundant free amino acid, is an important carrier and donor of nitrogen.^[18] Gln participates in the synthesis of various amino acids, and it is also the precursor of nucleotides and antioxidants

such as glutathione-SH (GSH). Adequate quantities of GSH can improve the antioxidant capacity, thereby protecting the liver cells against the damage induced by free radicals of oxygen. GSH can also inhibit the activity of nuclear factor kappa B, the release of related cytokines (e.g., TNF- α), and the aggregation of neutrophils.^[19,20] In this study, the levels of L-aspartic acid, amino adipic acid, L-glutamine, and glutathione in the MOD group were obviously disordered, but their levels were restored after the intervention of SCP, suggesting that SCP protects the liver by regulating amino acid metabolism and antioxidative mechanisms.

Arachidonic acid, a polyunsaturated essential fatty acid, is involved in the inflammatory response and immune system regulation. During the process of immunological liver injury, a large number of arachidonic acid is released, which can promote the secretion of neutrophils and inflammatory mediators, activate surface receptors, cause lipid peroxidation, and generate a large number of reactive oxygen species, which eventually leads to oxidative stress.^[21] Our results showed that the level of arachidonic acid was significantly reduced in the MOD group after the intervention of SCP.

CONCLUSION

In this study, an LC/MS-based metabolomics method was used to identify the metabolic regulation of SCP on the immunological liver injury induced by Con A in mice. According to our results, SCP might alleviate the oxidative stress and inflammatory reaction in the immunological liver injury, and alleviate the metabolic dysfunction caused by Con A. The possible metabolic pathways by which SCP acts are as follows: energy metabolism, amino acid metabolism, taurine metabolism, amino saccharide and nucleotide metabolism, arachidonic acid metabolism, and lipid metabolism (Figure 8). This research might be helpful in clarifying the prevention and treatment of immunological liver injury by SCP.

Financial support and sponsorship

This work was financially supported by the Natural Science Foundation of Jilin Province (No. 20170309006YY; 20170307016YY) and TCM science and technology project of Jilin Province (No. 2020119).

Conflicts of interest

There are no conflicts of interest.

REFERENCES

- Gao Y, Liu W, Wang W, Zhao X, Wang F. Polygluronate sulfate (PGS) attenuates immunological liver injury *in vitro* and *in vivo*. *Int J Biol Macromol* 2018;114:592-8.
- Nishida N, Kudo M. Liver damage related to immune checkpoint inhibitors. *Hepatol Int* 2019;13:248-52.
- Wang CM, Yuan RS, Zhuang WY, Sun JH, Wu JY, Li H, *et al.* Schisandra polysaccharide inhibits hepatic lipid accumulation by downregulating expression of SREBPs in NAFLD mice. *Lipids Health Dis* 2016;15:195.
- Yuan R, Tao X, Liang S, Pan Y, He L, Sun J, *et al.* Protective effect of acidic polysaccharide from *Schisandra chinensis* on acute ethanol-induced liver injury through reducing CYP2E1-dependent oxidative stress. *Biomed Pharmacother* 2018;99:537-42.
- Nowotny A. *Basic Exercises in Immunochemistry*. 2nd ed.. Switzerland: Springer; 1979.
- Murado MA, Vázquez JA, Montemayor MI, Cabo ML, del Pilar González M. Two mathematical models for the correction of carbohydrate and protein interference in the determination of uronic acids by the m-hydroxydiphenyl method. *Biotechnol Appl Biochem* 2005;41:209-16.
- Kruger NJ. The Bradford method for protein quantitation. *Methods Mol Biol* 1994;32:9-15.
- Li X, Xiong F, Liu Y, Liu F, Hao Z, Chen H. Total fractionation and characterization of the water-soluble polysaccharides isolated from *Enteromorpha intestinalis*. *Int J Biol Macromol* 2018;111:319-25.
- Nakagawasa O, Yamada K, Nemoto W, Sato S, Ogata Y, Miya K, *et al.* Liver hydrolysate attenuates the sickness behavior induced by concanavalin A in mice. *J Pharmacol Sci*

- 2015;127:489-92.
10. Ye T, Wang T, Yang X, Fan X, Wen M, Shen Y, *et al.* Comparison of concanavalin a-induced murine autoimmune hepatitis models. *Cell Physiol Biochem* 2018;46:1241-51.
 11. Ruat M, Chavarria L, Campreciós G, Suárez-Herrera N, Montironi C, Guixé-Muntet S, *et al.* Impaired endothelial autophagy promotes liver fibrosis by aggravating the oxidative stress response during acute liver injury. *J Hepatol* 2019;70:458-69.
 12. Huang TT, Zou Y, Corniola R. Oxidative stress and adult neurogenesis – Effects of radiation and superoxide dismutase deficiency. *Semin Cell Dev Biol* 2012;23:738-44.
 13. Kolac UK, Ustuner MC, Tekin N, Ustuner D, Colak E, Entok E. The anti-inflammatory and antioxidant effects of *salvia officinalis* on lipopolysaccharide-induced inflammation in rats. *J Med Food* 2017;20:1193-200.
 14. Yang Y, Li F, Wei S, Liu X, Wang Y, Liu H, *et al.* Metabolomics profiling in a mouse model reveals protective effect of Sancha granule on Con A-Induced liver injury. *J Ethnopharmacol* 2019;238:111838.
 15. Uzunhisarcikli M, Aslanturk A. Hepatoprotective effects of curcumin and taurine against bisphenol A-induced liver injury in rats. *Environ Sci Pollut Res Int* 2019;26:37242-53.
 16. Zhang H, Bai Y, Gao M, Zhang J, Dong G, Yan F, *et al.* Hepatoprotective effect of capsaicin against concanavalin A-induced hepatic injury via inhibiting oxidative stress and inflammation. *Am J Transl Res* 2019;11:3029-38.
 17. Holecek M. Ammonia and amino acid profiles in liver cirrhosis: Effects of variables leading to hepatic encephalopathy. *Nutrition* 2015;31:14-20.
 18. Kim MH, Kim H. The roles of glutamine in the intestine and its implication in intestinal diseases. *Int J Mol Sci* 2017;18:1051-66.
 19. Shrestha N, Chand L, Han MK, Lee SO, Kim CY, Jeong YJ. Glutamine inhibits CCl4 induced liver fibrosis in mice and TGF- β 1 mediated epithelial-mesenchymal transition in mouse hepatocytes. *Food Chem Toxicol* 2016;93:129-37.
 20. Hartmann R, Licks F, Schemitt EG, Colares JR, Da Silva J, Moura RM, *et al.* Effect of glutamine on liver injuries induced by intestinal ischemia-reperfusion in rats. *Nutr Hosp* 2017;34:548-54.
 21. Gai Z, Visentin M, Gui T, Zhao L, Thasler WE, Häusler S, *et al.* Effects of farnesoid X receptor activation on arachidonic acid metabolism, NF- κ B signaling, and hepatic inflammation. *Mol Pharmacol* 2018;94:802-11.